NASA TECHNICAL TRANSLATION NASA TT-20026 p. 29

# ANALYSIS OF THE FREE VIBRATION OF THE ROTATING DISK

R. Hashimoto, A. Nagamatsu and S. Michimura

Translation from National Aerospace Laboratory. Report. NAL-TR-546. November 1987. pp. 1-11.

(NASA-TT-20026) ANALYSIS OF THE FREE VIBRATION OF THE ROTATING DISK (NASA) 29 p N87-25609
Avail: NTIS HC A03/MF A01 CSCL 20K
Unclas
G5/39 0085580

NATIONAL AERONAUTICS AND SPACE ADMINISTRATION
WASHINGTON, D.C. 20546 JULY 1987

STANDARD TITLE PAGE

| 1. Report No. | 2. Government Accession No. | 3. Recipient's Catalog No. |
|---|---|---|
| NASA TT-20026 | | |

| 4. Title and Subtitle | 5. Report Date |
|---|---|
| Analysis of the free vibration of the rotating disk. | |
| | 6. Performing Organization Code |
| 7. Author(s) | 8. Performing Organization Report No. |
| Hashimoto, R. Nagamatsu, A., and Michimura S. | |
| | 10. Work Unit No. |
| 9. Performing Organization Name and Address | 11. Contract or Grant No. |
| Leo Kanner Associates<br>1800 Broadway<br>P. O. Box 5187<br>Redwood City, CA 94063 | NASw-4005 |
| | 13. Type of Report and Period Covered |
| | Translation |
| 12. Sponsoring Agency Name and Address | 14. Sponsoring Agency Code |
| National AEronautics and Space Administration<br>Washington, DC 20546 | |

15. Supplementary Notes

Translation from National Aerospace Laboratory, Tokyo, Japan. Report No. NAL-TR-546. November 1987. pp. 1-11
79N76956

16. Abstract

The vibration of the rotating disk is analyzed with the finite elemement method with consideration given to the effect of the centrifugal force. A fan-shaped element is proposed for the first time by the authors fo the analysis of both in-plane and bending deformations of the shell structure. The calculated results of the natural modes and their frequencies of a model disk are compared with the experimental ones, and the both results agree well quantitatively.

| 17. Key Words [Selected by Author(s)] | 18. Distribution Statement |
|---|---|
| | unclassified-unlimited |

| 19. Security Classif.(of this report) | 20. Security Classif. (of this page) | 21. No. of pages | 22. |
|---|---|---|---|
| UNCLASSIFIED | UNCLASSIFIED | 28 | |

# ANALYSIS OF THE FREE VIBRATION OF THE ROTATING DISK

Ryosaku HASHIMOTO, Akio NAGAMATSU and Seiichi MICHIMURA

Abstract

The vibration of the rotating disk analyzed with the finite element method with consideration given to the effect of the centrifugal force. A fan-shaped element is proposed for the first time by the authors for the analysis of both in-plane and bending deformations of the shell structure. The calculated result of the natural modes and their frequencies of a model disk are compared with the experimental ones, and the both results agree well quantatively.

## 1. INTRODUCTION

Along with the changes seen in rotational mechanical devices, eg. gas turbine engines ...etc. toward higher speed, lighter weight as well as larger size, the usage condition of the moving parts (rotary parts) is becoming more and more severe. At the time of designing rotary machinery, it is becoming increasingly important to understand not only the static characteristics of the rotary parts such as the distribution of the centrifugal stress but also some of the kinetic characteristics such as the specific cycle of vibration or the specific mode (both are called the specific pair). The objective of this research is to provide the above question with some basic data so that said specific pair of the optionally shaped rotating disks can be correctly grasped.

The analysis of the rotating disk has been accomplished in the past according to the method developed by Rayleigh-Ritz. It has become apparent, however, that the application of the existing method is difficult in the attempt to analyze the optionally shaped rotating disks. It is believed that the analysis based upon the limited element method is the most suitable for this purpose. In this study, the rotating disks are regarded as the shell structure consisting of the combination of the plane elements which receive the inner stress and the bending stress at the same time. According to this method, a new fan shaped element that is suitable for the analysis of the non-symmetric transformation of the symmetric shell structure as well as the analysis of vibration has been developed. Using the above described element, a program was prepared through the use of the limited element method in order to conduct the analysis of vibration considering the influence of the centrifugal force. Using the program, a sample question, a calculation on a simply shaped disk, has been solved. The answer which was compared with the result of the experiment has been found to be in perfect match.

## 2. ANALYSIS OF NUMERICAL VALUES THROUGH THE USE OF THE LIMITED ELEMENT METHOD

In this chapter, explanation of the non-symmetric variations of symmetric shell structures such as rotating disks or fan shaped structures which were newly developed in order to conduct the vibration analysis will be provided. Using the above described objects, a vibration analysis method which considers the increased rigidity by the centrifugal force is described.

Assuming that a rotating disk is a symmetric shell structure consisting of a number of plane elements which receive the inner stress and the bending stress simultaneously, deformation (of the symmetric shell structure) by the inner stress and by the bending stress can be considered separately as long as the extent of the deformation is minimal. Therefore, the rigidity matrix of this structure can be obtained by seeking the rigidity matrix of the inner element as well as the bending matrix of the bending element individually and by combining these two types of information.

Keys

$E$ : Young's coefficient

$\nu$ : Poisson's ratio

$h$ : thickness of the board

$\rho$ : density

$\omega$ : specific angle vibration number

$r\theta z$ : column coordinate system

$\xi\eta z$ : element coordinate system

$\begin{Bmatrix} U_r \\ U_\theta \end{Bmatrix}$ : displacement element within the surface

$\{N^P\}$ : displacement coefficient within the surface

$\{\delta^P\}$ : surface displacement of joint

$\{\epsilon^P\} = \begin{Bmatrix} \epsilon^P_r \\ \epsilon^P_\theta \\ r^P_{r\theta} \end{Bmatrix}$ : surface strain

$\{\sigma^P\}$ : surface stress

$\begin{Bmatrix} W_i \\ (\phi_r)_i \\ (\phi_\theta)_i \end{Bmatrix}$ : joint displacement by the bend of the joint i

$\{\delta^b\}$ : outer surface displacement of the joint

$[N^b]$ : outer surface displacement coefficient

$\{\epsilon^b\}$ : bending strain

$\{\sigma^b\} = \{M\} = \begin{Bmatrix} M_r \\ M_\theta \\ M_{r\theta} \end{Bmatrix}$ : bending stress (moment)

$[D^b]$ : bending elasticity matrix

$[m^P]$ : volume matrix (inner surface displacement)

$[m^b]$ : volume matrix (outer surface

displacement)

$[K^{P}]$ : rigidity matrix (inner surface displacement)

$[K^{b}]$ : rigidity matrix (outer surface displacement)

$\begin{Bmatrix} \epsilon_r^o \\ \epsilon_\theta^o \\ \gamma_{r\theta}^o \end{Bmatrix}$ : additional strain by the early stress

$\begin{Bmatrix} \sigma_r^o \\ \delta_\theta^o \\ \gamma_{r\theta}^o \end{Bmatrix}$ : early stress

$[G]$ : angular matrix

$[KG]$ : additional rigidity matrix

$\{F^b\}$ : equivalent joint force (outer surface disp.)

$\{F^P\}$ : equivalent joint force (inner surface disp.)

$[M]$ : total volume matrix

$[K]$ : total rigidity matrix

$\{\delta_o\}$ : joint amplitude vector

2.1 Inner surface rigidity

If we consider the fan shaped element as shown in Fig. 1, two displacement elements ($U_r$, $U_\theta$) must be present within one joint and the inner surface displacement must be decided by the figures of eight components without hesitation.

The most simplified formula which depicts the displacement toward the direction of the radius is as follows:

$$u_r = [1,\ \xi,\ \eta,\ \xi\eta]\{\alpha^P\} \tag{1}$$

The fixed number $\{\alpha^P\}$ can be shown in the following formulas using the conditions at the joint.

$$\begin{Bmatrix} u_{r1} \\ u_{r2} \\ u_{r3} \\ u_{r4} \end{Bmatrix} = \begin{bmatrix} 1 & 1 & 1 & 1 \\ 1 & 1 & 0 & 0 \\ 1 & 0 & 1 & 0 \\ 1 & 0 & 0 & 0 \end{bmatrix} \begin{Bmatrix} \alpha_1 \\ \alpha_2 \\ \alpha_3 \\ \alpha_4 \end{Bmatrix} \tag{2}$$

By solving the equation (2), $\{\alpha^P\}$ can be shown using the displacement $\{u\}$ as follows.

$$\begin{Bmatrix} \alpha_1 \\ \alpha_2 \\ \alpha_3 \\ \alpha_4 \end{Bmatrix} = \begin{bmatrix} 0 & 0 & 0 & 1 \\ 0 & 1 & 0 & -1 \\ 0 & 0 & 1 & -1 \\ 1 & -1 & -1 & 1 \end{bmatrix} \begin{Bmatrix} u_{r1} \\ u_{r2} \\ u_{r3} \\ u_{r4} \end{Bmatrix} \tag{3}$$

By applying the formula (3) to the formula (1), the following formula (Formula 4) can be formed:

$$u_r = [\xi\eta,\ \xi(1-\eta),\ (1-\xi)\eta,\ (1-\xi)(1-\eta)] \begin{Bmatrix} u_{r1} \\ u_{r2} \\ u_{r3} \\ u_{r4} \end{Bmatrix} \tag{4}$$

Fig. 1

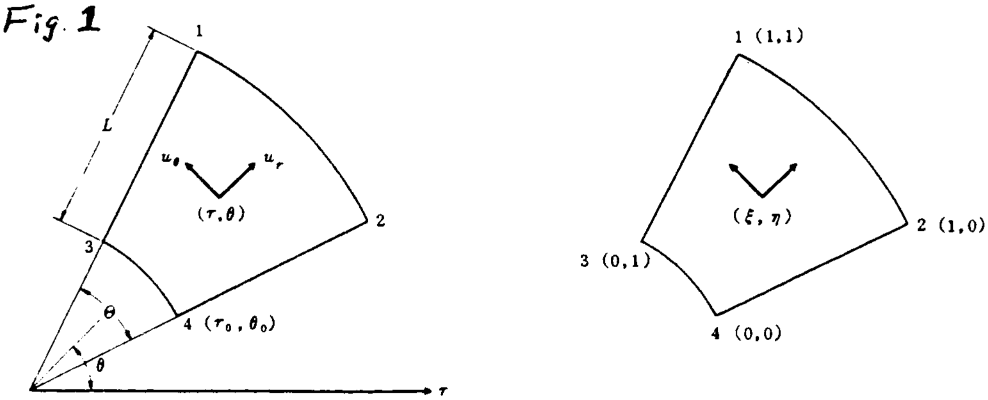


$(r,\theta)$ 座 標　　　　$(\xi,\eta)$ 座 標

図1　面内変位

The displacement ($U_\theta$) toward the direction of the circumference (of the circle) can also be obtained through the same method. Accordingly, the displacement coefficient of the element by the inner surface displacement can be shown according to the following formulas.

$$\begin{Bmatrix} u_r \\ u_\theta \end{Bmatrix} = \begin{bmatrix} \xi\eta & 0 & \xi(1-\eta) & 0 & (1-\xi)\eta & 0 & (1-\xi)(1-\eta) & 0 \\ 0 & \xi\eta & 0 & \xi(1-\eta) & 0 & (1-\xi)\eta & 0 & (1-\xi)(1-\eta) \end{bmatrix} \{\delta^p\}$$

$$= [N^p]\{\delta^p\} \qquad (5)$$

The strain at the optional points within the element can be determined by the following three components which contribute to the inner works.

$$\{\epsilon^p\} = \begin{Bmatrix} \varepsilon_r^p \\ \varepsilon_\theta^p \\ \gamma_{r\theta}^p \end{Bmatrix} = \begin{Bmatrix} \dfrac{\partial u_r}{\partial r} \\ \dfrac{u_r}{r} + \dfrac{\partial u_\theta}{r\partial\theta} \\ \dfrac{\partial u_r}{r\partial\theta} - \dfrac{u_\theta}{r} + \dfrac{\partial u_\theta}{\partial r} \end{Bmatrix}.$$

$$= \begin{bmatrix} 0 & 0 & 1 & 0 & 0 & 0 \\ 1/r & 0 & 0 & 0 & 0 & 1/r \\ 0 & -1/r & 0 & 1 & 1/r & 0 \end{bmatrix} \begin{Bmatrix} u_r \\ u_\theta \\ \dfrac{\partial u_r}{\partial r} \\ \dfrac{\partial u_\theta}{\partial r} \\ \dfrac{\partial u_r}{\partial \theta} \\ \dfrac{\partial u_\theta}{\partial \theta} \end{Bmatrix} \qquad (6)$$

From the Fig. 1, the following formula is established:

$$\begin{aligned} r &= r_0 + L\xi \\ \theta &= \theta_0 + \theta\eta \end{aligned} \tag{7}$$

If the formula (6) is re-written using the formulas (5) and (7), then it will become as follows:

$$\{\epsilon^p\} = \frac{1}{L}\frac{1}{\lambda}\begin{bmatrix} 0 & 0 & \lambda & 0 & 0 & 0 \\ 1 & 0 & 0 & 0 & 0 & \beta \\ 0 & -1 & 0 & \lambda & \beta & 0 \end{bmatrix}$$

$$\times \begin{bmatrix} [N^p] \\ \frac{\partial}{\partial\xi}[N^p] \\ \frac{\partial}{\partial\eta}[N^p] \end{bmatrix} \{\delta^p\} \tag{8}$$

However, Lambda and Beta can be determined through the following formula:

$$\lambda = r/L, \quad \beta = 1/\theta \tag{9}$$

$$[X] = \begin{bmatrix} 0 & 0 & \lambda & 0 & 0 & 0 \\ 1 & 0 & 0 & 0 & 0 & \beta \\ 0 & -1 & 0 & \lambda & \beta & 0 \end{bmatrix} \tag{10}$$

$$[Y] = \begin{bmatrix} [N^p] \\ \frac{\partial}{\partial\xi}[N^p] \\ \frac{\partial}{\partial\eta}[N^p] \end{bmatrix} \tag{11}$$

Then, the formula (8) can be re-written as follows:

$$\{\epsilon^P\} = \frac{1}{L}\frac{1}{\lambda}[X][Y]\{\delta^P\} \quad (12)$$

If $\{\epsilon P\} = [B^P]\{\delta P\}$, then [Bp] can be shown as follows from the formula (12).

$$\{\epsilon^P\} = [B^P]\{\delta^P\} \quad (13)$$

The formula which shows the relationship between the stress and the strain is as follows:

$\{\delta P\}$ indicates stress, $\{\epsilon P\}$ indicates strain, and [Dp] indicates the elasticity matrix as shown below:

$$[D^P] = \frac{E}{1-\nu^2}\begin{bmatrix} 1 & \nu & 0 \\ \nu & 1 & 0 \\ 0 & 0 & (1-\nu)/2 \end{bmatrix} \quad (16)$$

$$[B^P] = \frac{1}{L}\frac{1}{\lambda}[X][Y] \quad (14)$$

$$\{\sigma^P\} = [D^P]\{\epsilon^P\} \quad (15)$$

The rigidity matrix can be obtained as follows from the minimum condition of the entire potential energy:

$$[K] = \int [B]^T[D][B]\, d\,(\text{vol}) \quad (17)$$

$$[K^P] = h\iint \frac{1}{\lambda}[Y]^T[X]^T[D^P][X][Y]\,d\xi\, d\eta \quad (18)$$

If the thickness of the element is defined as h, and if the formulas (14) and (16) are substituted with the formula (17), the following formula which indicates the rigidity matrix of the element by the inner displacement can be formed.

## 2.2 Bending rigidity

Deformation by bending can be provided by the three components - outer vertical displacement Omega and two rotations $\phi_r$ and $\phi_\theta$.

The coefficient of the shape must be definable by the component of the joint displacement, in other words, by twelve parameters. Accordingly, assuming that:

$$\begin{aligned} w = {} & \alpha_1 + \alpha_2\xi + \alpha_3\eta + \alpha_4\xi^2 + \alpha_5\xi\eta + \alpha_6\eta^2 \\ & + \alpha_7\xi^3 + \alpha_8\xi^2\eta + \alpha_9\xi\eta^2 + \alpha_{10}\eta^3 + \alpha_{11}\xi^3\eta \\ & + \alpha_{12}\xi\eta^3 = [P]\{\alpha^b\} \end{aligned} \tag{19}$$

[P] can be shown as follows:

$$[P] = [1,\ \xi,\ \eta,\ \xi^2,\ \xi\eta,\ \eta^2,\ \xi^3,\ \xi^2\eta,\ \xi\eta^2,\ \eta^3,\ \xi^3\eta,\ \xi\eta^3] \tag{20}$$

If the displacement of Omega and the rotation are indicated by the joint displacement vector at the joint i, then the following formula can be established:

$$\{\delta_i^b\} = \begin{Bmatrix} w_i \\ (\phi_r)_i \\ (\phi_\theta)_i \end{Bmatrix} = \begin{Bmatrix} w_i \\ \left(\dfrac{\partial w}{r\partial\theta}\right)_i \\ -\left(\dfrac{\partial w}{\partial r}\right)_i \end{Bmatrix} \tag{21}$$

From the Fig. 2, Gamma and Theta can be shown in the following formulas:

$$\begin{aligned} r &= r_0 + L\xi \\ \theta &= \theta_o + \Theta\eta \end{aligned} \tag{22}$$

The following formula can be obtained by substituting the formula (22) with the formula (21):

$$\begin{aligned} \{\delta_i^b\} &= \begin{Bmatrix} w_i \\ \left(\dfrac{\partial w}{r\partial\theta}\right)_i \\ -\left(\dfrac{\partial w}{\partial r}\right)_i \end{Bmatrix} \\ &= \begin{bmatrix} 1 & 0 & 0 \\ 0 & \dfrac{1}{\Theta r_i} & 0 \\ 0 & 0 & -\dfrac{1}{L} \end{bmatrix} \begin{Bmatrix} w_i \\ \left(\dfrac{\partial w}{\partial \eta}\right)_i \\ \left(\dfrac{\partial w}{\partial \xi}\right)_i \end{Bmatrix} \end{aligned} \tag{23}$$

The formula (23) can be re-written as follows:

$$\{\delta_i^b\} = [a_i]^{-1}\{\delta_i'^b\} \tag{24}$$

Note: $[a_i]$ and $\{\delta_2'^b\}$ can be replaced by the following:

$$[a_i]=\begin{bmatrix} 1 & 0 & 0 \\ 0 & \theta r_i & 0 \\ 0 & 0 & -L \end{bmatrix},$$

$$\{\delta_i^{b}\}=\begin{Bmatrix} w_i \\ (\frac{\partial w}{\partial \eta})_i \\ (\frac{\partial w}{\partial \xi})_i \end{Bmatrix} \qquad (25)$$

If the formula (19) is substituted with (24), then the following formula can be obtained:

$$\{\delta_i^b\}=[a_i]^{-1}\begin{bmatrix} [P]_i \\ (\frac{\partial}{\partial \eta}[P])_i \\ (\frac{\partial}{\partial \xi}[P])_i \end{bmatrix}\{a^b\}$$

$$=[a_i]^{-1}[c_i]^{-1}\{a^b\} \qquad (26)$$

The total joint displacement can be shown as follows using the formula (26):

$$\{\delta^b\}=\begin{Bmatrix} \delta_1^b \\ \delta_2^b \\ \delta_3^b \\ \delta_4^b \end{Bmatrix}=[A]^{-1}[C]^{-1}\{a^b\} \qquad (27)$$

Note: $[A]$ and $[C]^{-1}$ can be shown in the following formulas:

$$[A]=\begin{bmatrix} [a_1] & 0 & 0 & 0 \\ 0 & [a_2] & 0 & 0 \\ 0 & 0 & [a_3] & 0 \\ 0 & 0 & 0 & [a_4] \end{bmatrix}.$$

$$[C]^{-1}=\begin{bmatrix} [c_1]^{-1} \\ [c_2]^{-1} \\ [c_3]^{-1} \\ [c_4]^{-1} \end{bmatrix}$$

Fig. 2 Bending displacement

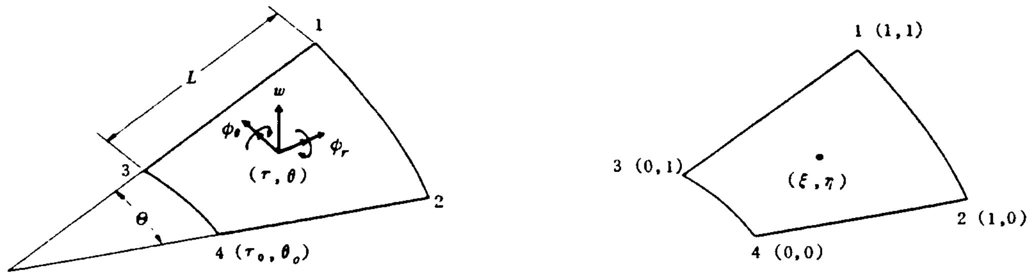


$(r,\theta)$ 座 標　　　　$(\xi,\eta)$ 座 標

図2 曲げ変位

The formula (27) is solved and $\{d^b\}$ is obtained as follows:

$$\{a^b\}=[C][A]\{\delta^b\} \tag{28}$$

The displacement within the element shown as the displacement at four joints is as follows:

$$w=[P]\{a^b\}=[P][C][A]\{\delta^b\}=[N^b]\{\delta^b\} \tag{29}$$

Accordingly, the displacement coefficient which receives the effect of bending is shown in the following formula:

$$[N^b]=[P][C][A] \tag{30}$$

The bending strain can be shown in the following three ratios as shown next:

$$\{\epsilon^b\}=\begin{Bmatrix} -\dfrac{\partial^2 w}{\partial r^2} \\ -\dfrac{\partial^2 w}{r^2\partial\theta^2} - \dfrac{\partial w}{r\,\partial r} \\ -2\dfrac{\partial^2 w}{r\partial\theta\partial r} + 2\dfrac{\partial w}{r^2\partial\theta} \end{Bmatrix} \tag{31}$$

Generalized stress in opposition to the above can be obtained by the following formula:

$$\{\sigma^b\} = \{M\} = \begin{Bmatrix} M_r \\ M_\theta \\ M_{r\theta} \end{Bmatrix} = [D^b]\{\epsilon^b\} \quad (32)$$

If the thickness is h and the Poisson's ratio is v, then the following formula can be established:

$$[D^b] = \frac{E h^3}{12(1-\nu^2)} \begin{bmatrix} 1 & \nu & 0 \\ \nu & 1 & 0 \\ 0 & 0 & (1-\nu)/2 \end{bmatrix} \quad (33)$$

The formula (31) can be re-written through the use of Lambda = Gamma/ L, Beta = 1 / Theta as follows:

$$\{\epsilon^b\} = -\frac{1}{L^2}\frac{1}{\lambda^2} \begin{bmatrix} \lambda^2 & 0 & 0 & 0 & 0 \\ 0 & \beta^2 & 0 & \lambda & 0 \\ 0 & 0 & 2\lambda\beta & 0 & 2\beta \end{bmatrix} \times \begin{Bmatrix} \partial^2 w/\partial\xi^2 \\ \partial^2 w/\partial\eta^2 \\ \partial^2 w/\partial\xi\partial\eta \\ \partial w/\partial\xi \\ \partial w/\partial\eta \end{Bmatrix} = -\frac{1}{L^2}\frac{1}{\lambda^2}[X^b] \times \begin{Bmatrix} \partial^2 w/\partial\xi^2 \\ \partial^2 w/\partial\eta^2 \\ \partial^2 w/\partial\xi\partial\eta \\ \partial w/\partial\xi \\ \partial w/\partial\eta \end{Bmatrix} \quad (34)$$

From the formula (19), the following formulas can be established:

$$\begin{Bmatrix} \partial^2 w/\partial\xi^2 \\ \partial^2 w/\partial\eta^2 \\ \partial^2 w/\partial\xi\partial\eta \\ \partial w/\partial\xi \\ \partial w/\partial\eta \end{Bmatrix} = \begin{bmatrix} \partial^2[P]/\partial\xi^2 \\ \partial^2[P]/\partial\eta^2 \\ \partial^2[P]/\partial\xi\partial\eta \\ \partial[P]/\partial\xi \\ \partial[P]/\partial\eta \end{bmatrix} \{\alpha^b\} = [Y^b]\{\alpha^b\} \quad (35)$$

By substituting the formula (34) with the formulas (28) and (35), the following formula can be established:

$$\{\epsilon^b\} = -\frac{1}{L^2}\frac{1}{\lambda^2}[X^b][Y^b][C][A]\{\delta^b\} \tag{36}$$

By re-writing the formula which indicates the strain and displacement as $\{\epsilon^b\} = [B^b]\{\delta^b\}$ (37), the following formula can be established from the formula (36):

$$[B^b] = -\frac{1}{L^2}\frac{1}{\lambda^2}[X^b][Y^b][C][A] \tag{38}$$

The rigidity matrix by bending can be shown as follows provided that the thickness of the element is fixed within the element:

$$\begin{aligned}[K^b] &= \iint [B^b]^T [D^b][B^b]\, r\, d\theta\, dr \\ &= \frac{\theta}{L^2}[A][C]^T \iint \frac{1}{\lambda^3}[Y^b]^T[X^b]^T \\ &\quad \times [D^b][X^b][Y^b]\, d\xi\, d\eta\, [C][A]\end{aligned} \tag{39}$$

## 2.3 Mass matrix

The general formula of the mass matrix is shown as follows:

$$[m] = \int [N]^T \rho [N]\, d(\text{vol}) \tag{40}$$

In the above formula, [N] and Rho indicate the displacement coefficient and density respectively.

The mass matrix, according to the same manner as the rigidity matrix, may be gained by combining the matrix obtained by the inner surface displacement and the bending displacement, which are separately obtained. The mass matrix by the inner surface displacement is as follows through the use of the formulas (40), (5) and (7):

$$[m^p] = \rho h L^2 \theta \int_t^{t+1} \lambda \left( \int_0^1 [N^p]^T [N^p] d\eta \right) d\lambda \tag{41}$$

It must be noted that the thickness of the element (h) is fixed and that t and Lambda are defined as follows:

$$t = r_0 / L \quad , \quad \lambda = r / L = t + \xi$$

The mass matrix by bending can be obtained as follows through the use of the formulas (40), (30) and (22).

$$[m^b] = \rho h L^2 \theta [A][C]^T \int_0^1 \int_0^1 (\xi + t) \times [P]^T [P] d\xi d\eta [C][A] \tag{42}$$

## 2.4 Influence of the centrifugal force

The shape of rotating disks will be changed by the centrifugal force at the time of rotation. At this time, it is assumed that the inner surface stress $\{\sigma_0\}$ is influenced by the external displacement (Omega). If the same problem is treated according to the linear mode, the external displacement will generate additional expansion at the center plane of the board toward the direction of the radius and the circumference (of a circle). The displacement toward the radius direction (dr) changes to dr'.

$$dr' = \sqrt{1 + \left(\frac{\partial w}{\partial r}\right)^2} \, dr = \left\{ 1 + \frac{1}{2}\left(\frac{\partial w}{\partial r}\right)^2 + \cdots\cdots \right\} dr \tag{43}$$

Accordingly, the additional strain toward the radius direction will be as follows:

$$\epsilon_r^o = \frac{1}{2}\left(\frac{\partial w}{\partial r}\right)^2 \qquad (44)$$

$$\epsilon_\theta^o = \frac{1}{2}\left(\frac{\partial w}{r\partial\theta}\right)^2 \qquad (45)$$

In the same manner, the strain toward the circumference (of the circle) and the shear strain will become as shown below:

$$\gamma_{r\theta}^o = \left(\frac{\partial w}{\partial r}\right)\left(\frac{\partial w}{r\partial\theta}\right) \qquad (46)$$

Fig. 3 Increase in the length of the neutral plane by the side displacement

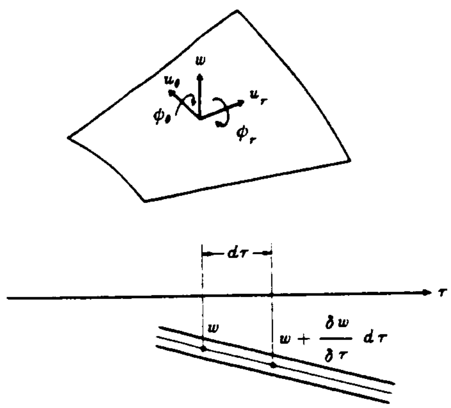


図3 横変位による中立面長さの増加

Through the generation of the strain as described above, the per fixed cubic measurement potential energy by the inner surface early stress (centrifugal force) will be increased by:

$$\frac{1}{2}\sigma_r^o\left(\frac{\partial w}{\partial r}\right)^2 + \frac{1}{2}\sigma_\theta^o\left(\frac{\partial w}{r\partial\theta}\right)^2 + \tau_{r\theta}^o\left(\frac{\partial w}{\partial r}\right)\left(\frac{\partial w}{r\partial\theta}\right) \qquad (47)$$

The above formula can also be re-written as:

$$\frac{1}{2}\begin{Bmatrix}\frac{\partial w}{\partial r}\\ \frac{\partial w}{r\partial\theta}\end{Bmatrix}^T\begin{bmatrix}\sigma_r^o & \tau_{r\theta}^o\\ \tau_{r\theta}^o & \sigma_\theta^o\end{bmatrix}\begin{Bmatrix}\frac{\partial w}{\partial r}\\ \frac{\partial w}{r\partial\theta}\end{Bmatrix}=\frac{1}{2}\begin{Bmatrix}\frac{\partial w}{\partial r}\\ \frac{\partial w}{r\partial\theta}\end{Bmatrix}^T \times [\sigma_o]\begin{Bmatrix}\frac{\partial w}{\partial r}\\ \frac{\partial w}{r\partial\theta}\end{Bmatrix} \quad (48)$$

Noticing that the angle of the incline of the board is equal to the coefficient of the joint displacement, the following formula can be established concerning the additional potential energy of the entire element:

$$\begin{Bmatrix}\frac{\partial w}{\partial r}\\ \frac{\partial w}{r\partial\theta}\end{Bmatrix}=[G]\{\delta^b\} \quad (49)$$

From the above formula, the additional rigidity matrix will become as follows:

$$\frac{1}{2}\{\delta^b\}^T[K_G]\{\delta^b\} \quad (50)$$

$$[K_G]=\iiint[G]^T\begin{bmatrix}\sigma_r^o & \tau_{r\theta}^o\\ \tau_{r\theta}^o & \sigma_\theta^o\end{bmatrix}[G]\,r\,dr\,d\theta\,dz = h\iint[G]^T[\sigma_o][G]\,r\,d\theta\,dr \quad (51)$$

The incline angle matrix [G] can be established using the formula [29] and the formula shown below. From the Fig. 2, the following formulas are set up first:

$$r=r_0+L\xi \quad , \quad \theta=\theta_o+\theta\eta$$

From the above formulas, the following formulas are established:

$$\begin{Bmatrix}\frac{\partial w}{\partial r}\\ \frac{\partial w}{r\partial\theta}\end{Bmatrix}=\begin{bmatrix}\frac{1}{L} & 0\\ 0 & \frac{1}{\theta r}\end{bmatrix}\begin{Bmatrix}\frac{\partial w}{\partial\xi}\\ \frac{\partial w}{\partial\eta}\end{Bmatrix}=\frac{1}{L\lambda}\begin{bmatrix}\lambda & 0\\ 0 & \beta\end{bmatrix}\begin{Bmatrix}\frac{\partial w}{\partial\xi}\\ \frac{\partial w}{\partial\eta}\end{Bmatrix}=\frac{1}{L\lambda}[T]\begin{Bmatrix}\frac{\partial w}{\partial\xi}\\ \frac{\partial w}{\partial\eta}\end{Bmatrix} \quad (52)$$

From the formulas (20) and (29), the following formula can be established:

$$\begin{Bmatrix} \dfrac{\partial w}{\partial \xi} \\ \dfrac{\partial w}{\partial \eta} \end{Bmatrix} = \begin{Bmatrix} \dfrac{\partial [P]}{\partial \xi} \\ \dfrac{\partial [P]}{\partial \eta} \end{Bmatrix} [C][A]\{\delta^b\}$$

$$= [G'][C][A]\{\delta^b\} \qquad 53$$

From the formulas (52) and (53), the following formula can be set up:

$$\begin{Bmatrix} \dfrac{\partial w}{\partial r} \\ \dfrac{\partial w}{r \partial \theta} \end{Bmatrix} = \frac{1}{L\lambda}[T][G'][C][A]\{\delta^b\} = [G]\{\delta^b\}$$

$$54$$

From the formulas (51) and (54), the additional rigidity matrix can be obtained according to the following manner:

$$[K_G] = h\,\theta\,[A][C]^T \iint [G']^T[T][\sigma_o]$$
$$\times [T][G']\frac{1}{\lambda}d\xi\, d\eta [C][A] \qquad 55$$

[Note] The inner surface force ($[\sigma_o]$) can be obtained from the formulas (12) and (15) using the following formula:

$$\begin{Bmatrix} \sigma_r^o \\ \sigma_\theta^o \\ \tau_\eta^o \end{Bmatrix} = \frac{1}{L}\frac{1}{\lambda}[D^p][X^p][Y^p]\{\delta^p\} \qquad 56$$

2.5 The constant nodal point force by the centrifugal force

According to the finite element method, the stress on the boundary that is applied to the element or the distributional load within the element can be defined as the statically equivalent joint force. In other words, the equivalent joint force $\{Fp\}$ is shown by the following formulas provided that the distributional load within the element is given the value of $\{p\}$.

$$\{F_p\} = -\int [N]^T \{p\} d(\mathrm{vol}) \qquad 57$$

From the Fig. 4, the distributional load by the centrifugal force is shown as follows:

$$\begin{aligned} f_r &= \rho\tau'\omega^2 \cos\phi = \rho\omega^2 L\,(t+\xi)\cos^2\phi \\ f_\theta &= 0 \qquad\qquad\qquad\qquad\qquad 58 \\ f_z &= \rho\tau'\omega^2 \sin\phi = \rho\omega^2 L\,(t+\xi)\cos\phi\,\sin\phi \end{aligned}$$

[Note] Rho = density; Omega = angular speed; t = Delta o/ L; Tau = Tau o + L Xi.

The inner surface equivalent joint force is obtained by substituting the formulas (5) and (58) with the formula (57).

$$\begin{aligned} \{F_p\} &= -h\iint [N^p]^T \begin{Bmatrix} f_r \\ f_\theta \end{Bmatrix} \tau\, d\theta\, d\tau \\ &= -\rho\omega^2 h\,\theta\, L^3 \cos^2\phi \iint [N^p]^T \begin{Bmatrix} (t+\xi)^2 \\ 0 \end{Bmatrix} d\xi\, d\eta \end{aligned} \qquad 59$$

The formula (59) indicates the equivalent joint force by the centrifugal force within the surface. The equivalent joint force by the centrifugal force outside the surface is also obtained by substituting the formulas (30) and

(58) witn the formula (57).

$$\{F_b\} = -h \iint [N_b]^T \{f_z\} r\, d\theta\, dr$$
$$= -\rho\omega^2 h\, \Theta\, L^3 \cos\phi \sin\phi [A][C]^T$$
$$\times \iint [P]^T (t+\xi)^2\, d\xi\, d\eta \qquad (60)$$

The formula (60) indicates the equivalent joint force by the centrifugal force outside the surface.

2.6 The problem of the characteristic value

Through the method described up to the previous chapter, the rigidity matrix and the mass matrix are obtained, and the following kinetic equation can be established. [Note] [M] indicates the mass matrix, and [K] indicates the rigidity matrix.

$$[M]\{\ddot{\delta}\} + [K]\{\delta\} = 0 \qquad (61)$$

Since the entire points of the system move according to the same phase in free oscillation, the following formula can be set up:

$$\{\delta\} = \{\delta_o\} \sin\omega t \qquad (62)$$

From the above formula, the following formula can be established:

$$\{\ddot{\delta}\} = -\omega^2 \{\delta_o\} \sin\omega t \qquad (63)$$

By substituting the formula (62) with (61), the following formula of the characteristic value problem can be established provided that $\{\delta_0\} \neq 0$ :

$$|[K] - \omega^2 [M]| = 0 \qquad (64)$$

The above characteristic value problem was solved using the sub-space repetition method in order to obtain the individual pair.

Fig. 4 The centrifugal force applied to the element

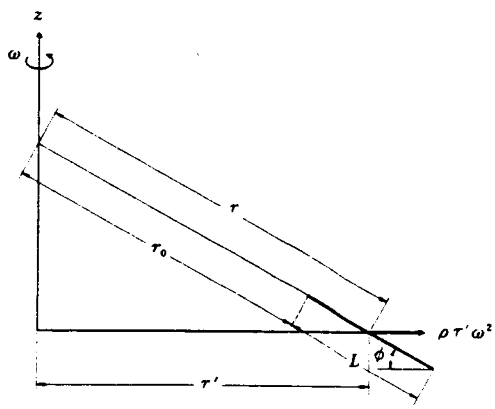


図4 要素に作用する遠心力

Fig. 5 Schematic chart of the experiment

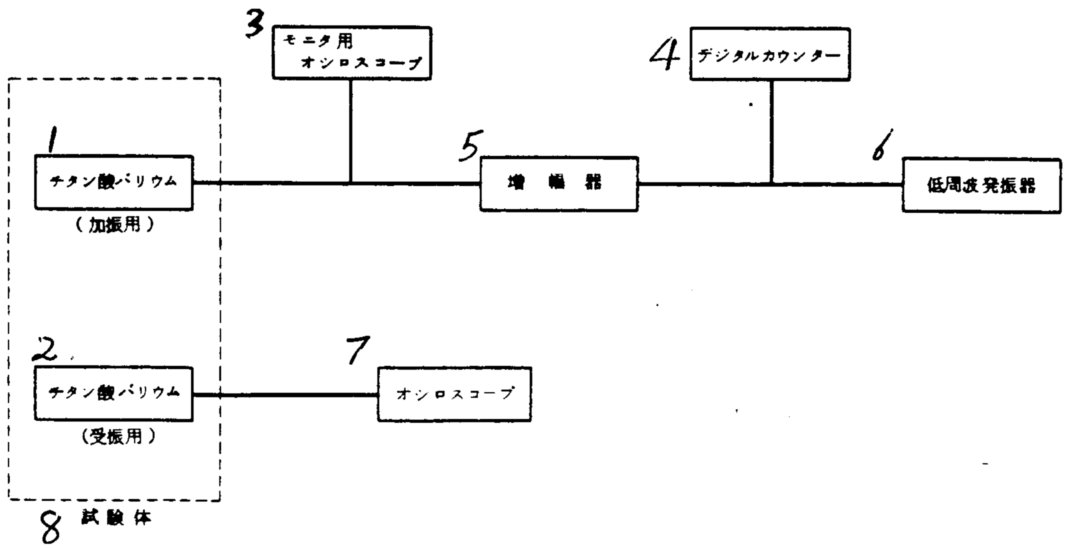


図5 実験の概略図

1. titanic acid barium (for oscillation) 2. titanic acid barium (for receiving) 3. an oscilloscope for monitoring 4. a digital counter 5. an amplifier 6. a low frequency

oscillator 7. an oscilloscope 8. a test body

Fig. 6 Oscillation mode

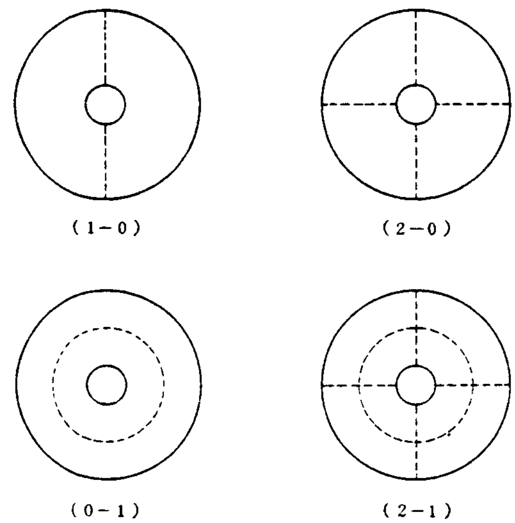


図6 振動モード

## 3. METHOD OF THE EXPERIMENT

The experiment was carried out according to the schematic chart shown in Fig. 5. In other words, a pressure element (a titanic acid barium magnetic piece) is attached to the rotating disk at the location (at the center of the rotating disk) where the bend moment in primary vibration mode is the highest. The vibration strain that is generated as the result is detected by the piezoelectric element. What has been detected by the piezoelectric element is changed into electric signal, and the waveform of the electric signal is observed by an oscilloscope in order to obtain the natural oscillation. The vibration mode was observed through the oscillation chart.

The vibration mode that is obtained by the experimentation is shown in (n-s) form in Fig. 6. The n indicates the number of the joints, and the s indicates the number of the joining circles.

## 4. COMPARISON AND DISCUSSION OF THE RESULT OF THE CALCULATION AND THE EXPERIMENT

Experiment and calculation were carried out for the disk that is shown in Tab. 1 and Fig. 7(A) of which inner circumference is immobilized. The number of the natural oscillation that is obtained as the result is shown in Tab. 2. According to the Tab. 2, the actual (experimental) figure and the theoretical figure of the natural oscillation are almost the same. Yet, the number of the oscillation at the ninth attempt shows higher discrepancies (approximately 10 %). This is thought to be due to the rough division of the element. If the high degree of natural pair with complex oscillation mode is to be obtained, it is believed that the element division that is carried out in detail is the est answer. The calculation was done using the element division (60 elements, 70 joints) as shown in Fig. 8.

The experiment was done on the plane board as shown in Fig. 7 (A). It must be noted that the shapes as shown in (B) and (C) can also be analyzed using the program prepared as a part of this experimentation. Its result is shown in Tab. 3. According to the result, the disks shaped like (B) or (C) have less number of natural oscillation compared with the disks of (A) shape.

Next, a calculation was done on the influence of the centrifugal force. The result is shown in Tab. 4. The natural oscillation at the time of rotation showed higher level (of natural oscillation) than at the time of immobilized condition. This is thought to be due to the increased rigidity due mainly to the centrifugal force.

Tab. 1 Nature of the disk

| | |
|---|---|
| Material | Aluminum board (plate) |
| Young's coefficient | 7200Kg/ square mm |
| Density | 0.2755 x 10 kg sec / mm |
| Poisson's ratio | 0.33 |
| Thickness of the board | 2.0 mm |
| Outer radius | 150 mm |
| Inner radius | 30 mm |

Tab. 2 Calculation and experiment figures

表2 計算値と実験値

| 1 振動次数 | 2 計算値(Hz) | 3 実験値(Hz) | 4 モード形(n−s) |
|---|---|---|---|
| 1 | 104 | 107 | (1 − 0) |
| 2 | 115 | 113 | (0 − 0) |
| 3 | 136 | 153 | (2 − 0) |
| 4 | 276 | 291 | (3 − 0) |
| 5 | 492 | 494 | (4 − 0) |
| 6 | 717 | 719 | (0 − 1) |
| 7 | 743 | 776 | (1 − 1) |
| 8 | 745 | 735 | (5 − 0) |
| 9 | 857 | 930 | (2 − 1) |

5 (n：節線の数，s：節円の数)

1. Oscillation # 2. Calculated figures 3. Experimentation figures 4. shape of the mode (n-s) 5. (n: number of the joint; s: number of the joining circle)

Tab. 3 Calculation figures

表3 計 算 値

| 1 振動次数 | A (Hz) | B(Hz) | C (Hz) |
|---|---|---|---|
| 1 | 104 | 98 | 83 |
| 2 | 115 | 109 | 92 |
| 3 | 136 | 133 | 129 |
| 4 | 276 | 275 | 274 |
| 5 | 492 | 491 | 489 |
| 6 | 717 | 674 | 573 |
| 7 | 743 | 703 | 605 |
| 8 | 745 | 744 | 734 |
| 9 | 857 | 821 | 739 |

1. Oscillation #

Tab. 4 Number of the first natural oscillation during rotation

(for the figure shown in Fig. 7 (A) )

| | | | | |
|---|---|---|---|---|
| 回転数(R.P.M.) 1 | 0 | 2500 | 5000 | 7500 |
| 一次固有振動数(Hz) 2 | 104 | 114 | 140 | 175 |

1. RPM 2. number of the first natural oscillation

Fig. 7 Cross sectional figure of the rotation disk

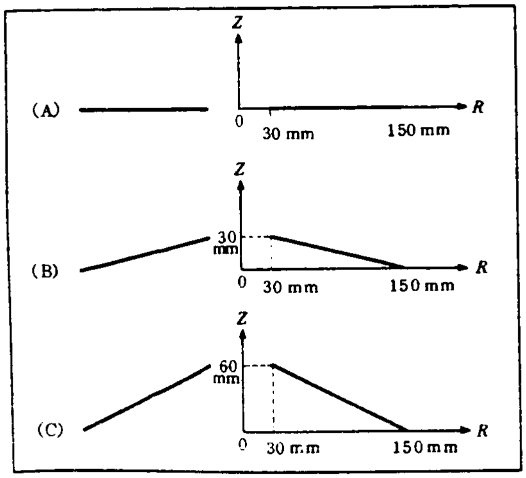


図7 翼車の断面図

Fig. 8 Division of the element

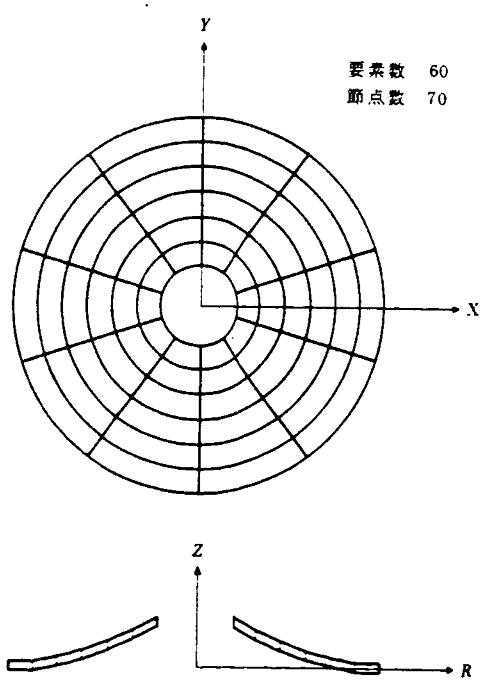


図8 要素分割

## 5. CONCLUSION

The following conclusion has been obtained as the result of this experiment:

1. Considering rotation disks of optional shapes as shell structures, a fan shaped board element which receives the inner surface force as well as the bend effect simultaneously has been developed. Using the above element, a program to attain the natural pair has been developed.

2. Oscillation test of the rotating disk was carried out. The result of the test and the calculation matched well.

3. Although the experimentation was carried out on models with rather simple shapes, the above described program can be applied to analyze the oscillation of disk shaped or cone shaped devices such as compressors, turbines and others which have more complex shapes.

## Bibliography

1. Zienkiewicz, O. C., The Finite Element Method in Engineering Science, (1971), McGraw-Hill, (Translated by M. Yoshiori, K. Yamada, Kisokogaku ni okeru Matrix yugen yosoho, (1975), Baifukan)

2. K. Yamada, T. Sato, Yugen yosoho ni okeru saikin no koyuchi mondai kaiho, Production Research, Vol. 26, No. 6, (1974, 6)